ELECTROSPINNING PREPARATION AND LUMINESCENE PROPERTIES OF CaTiO$_3$: RE (Eu^{3+}/Gd^{3+}) NANOFIBERS

Q. LI^{a*}, R. YAN^a, L. M. DONG^a, Y. F. ZHANG^b

^{a}College of Materials Science and Engineering, Harbin University of Science & Technology Harbin, China
^{b}AECC Harbin Dongan Engine Co.,LTD. , Harbin, China

One dimension CaTiO$_3$: Eu^{3+}, Gd^{3+} nanofibers have been prepared by a combination method of sol-gel process and electrospinning. X-ray diffraction (XRD), scanning electron microscopy (SEM), thermogravimetric and differential thermal analysis (TG-DTG), and photoluminescence (PL) properties were used to characterize the resulting samples. SEM results indicate the surface the as-formed fibers are rough, and the as-prepared nanofibers consist of nanoparticles. The photoluminescence properties exhibit that the obtained phosphors can be efficiently excited in the range from 370 to 420 nm. Under 398nm excitation, the phosphors show the characteristic emission of Eu^{3+}, i.e. ^5D_o-$^7F_1$、 ^5D_o-$^7F_2$、 ^5D_o-$^7F_3$ transitions. A certain amount of Gd^{3+} and Eu^{3+} is contributed to the intensity of light emission.

1. Introduction

As a new generation of solid light source, White light-emitting diodes（white LEDs）has the advantages of small size, fast response, environment friendness，long service life, etc., so it can be widely used in various industries. At present, the commercial white LED is widely used by the combination of blue GaN LED chip and yellow YAG:Ce phosphor, which has a very high luminous efficiency. But it cannot satisfy the optimum requirements. The lack of a red-light component leads to a high correlated color temperature (7765 K) and a poor color-rendering index, which restricts its broader application [1]. In addition to this method, another kind of w-LED can be fabricated by combining the GaN-based blue chip with green and red phosphors or via coupling of a UV LED (350−420 nm) with blue, green, and red phosphors [2-4]. Among them, red fluorescent powder is an important additive to adjust the color index. At present, the Eu^{3+}-doped Y$_2$O$_3$ is most commercialized. However, it usually exhibits a narrow peak and strong absorption at 254 and 393 nm, which restrict its applications in matching NUV chips [5]. In addition, the red phosphors for ultraviolet (UV) LED chip such as Y$_2$O$_2$S:Eu^{3+} or CaS: Eu^{2+} have weak luminescence, and these sulfide-based red phosphors have poor chemical stability [6, 7]. Therefore, novel red-emitting phosphors with high luminous efficiency and stable performance under facial or mild synthesis conditions are still in great need.

The titanate system as a red fluorescent powder has been widely concerned. On the one hand, due to its good chemical and thermal stability, on the other hand, it is due to the anionic group in the matrix to play a certain role in sensitization, can effectively absorb the excitation energy and transfer to the rare earth ions to make it shine. At the same time, rich resources of

---

*Corresponding author: qinalily@163.com

titanium lead to the clear price advantage compared with other molybdate and Tungstate. All these provide favorable conditions for the research and development of rare earth titanate luminescent materials.

Up to now, there have been many methods reported for the synthesis of titanate luminescent materials with different compositions, including a high-temperature solid-state reaction rout [8，9], co-precipitation [10], and sol-gel method [11]. In comparison to these methods, electrospinning is a simple, convenient, cost-effective, and versatile technique for generating long fibers with diameters ranging from tens of nanometers up to micrometers. The fibers prepared by electrospinning have good orientation, a large specific surface area, a large aspect ratio, and dimensional stability, which can be applied in sensors, electronic and optical devices, biomedical fields, and catalyst supports. [12]

In this study, the $CaTiO_3$: Eu^{3+} nanofibers are synthesized by electrospinning method, and their luminescent properties were investigated.

2. Materials and methods

2.1. Materials Preparation.

Nanofibers of $CaTiO_3$: Eu^{3+} phosphors were prepared by a method of sol-gel process and electrospinning. The stoichiometric amounts of $Ca(NO_3)_2$ and Eu_2O_3 (EP, Tianjin Guangfu Fine Chemical Research Institute) were dissolved in acetic acid (AR), and Tetrabutyl titanate ($\geqq 98.0\%$, Tianjin Guangfu Fine Chemical Research Institute) was dissolved in ethanol, and then all the solutions were mixed with a ethanol solution containing a certain amount of poly(vinylpyrrolidone) (PVP, Mw =30000, Tianjin Zhiyuan Chemical Reagen Co.ltd) and N'N-dimethylformamide (DMF). The mixed solution was stirred for 4 h to obtain a homogeneous hybrid sol for further electrospinning. In order to obtain the precursor solution with different concentration of Gd^{3+}, different amount of gadolinium oxide (EP, Tianjin Guangfu Fine Chemical Research Institute) were weighed and dissolved in acetic acid (AR) and added into the mixed solution.

The precursor solution was transferred into the spinneret (a metallic needle), and the distance between the spinneret and collector (a grounded conductor) was fixed at 14 cm, and the high-voltage supply was maintained at 31 kV. The as-prepared hybrid precursor samples were annealed to the desired temperature (600-1000 °C) and held there for 4 h in air. Finally $CaTiO_3$: Eu^{3+} nanofibers were obtained.

2.2 Measurement Characterization.

The structures of the phosphor were established by X-ray diffractometer (XRD) (Shimadzu, XRD-6000, Cu Ka target) and the morphology of the particles was observed by field emission scanning electron microscope (FE-SEM) (Sirion 200, Philip). The thermal behavior was studied by differential thermal analysis and thermogravimetric analysis (TG) on simultaneous thermal analyses (N5350030, Perkin Elmer). TG and DTA measurements were performed up to $650\,^{o}C$ in air at a heating rate of $10\,^{o}C$ min^{-1}. The photoluminescence properties of the phosphors were studied on fluorescence spectrophotometer (Shimadzu, model RF-5301 PC). All the photoluminescence properties of the phosphors were measured at room temperature.

3. Results and discussion

3.1 Phase Identification and Crystal Structure

Fig. 1 shows the representative XRD patterns of $CaTiO_3$:$0.07Eu^{3+}$ samples annealed from 600 to $1000^{o}C$ as well as the JCPDS card (no. 22-153) for $CaTiO_3$. When the precursor sample is

calcined at 600°C (Figure 1a), some weak and broad peaks at 2θ 33.10°、47.44°、59.06° and 69.28° are present, which are due to the (1 2 1) 、(0 4 0) 、(2 4 0) and (2 4 2) reflections of the crystalline $CaTiO_3$, respectively.
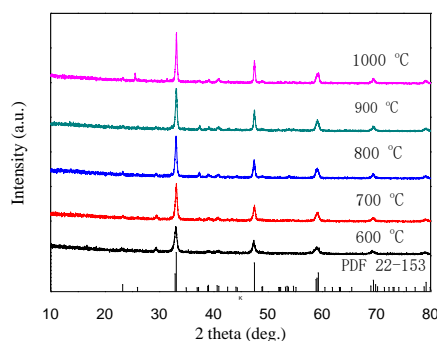
Fig. 1: Representative XRD patterns of 7mol% Eu^{3+} doped $CaTiO_3$ samples synthesized at 600-1000°C for 4h. The standard card data of $CaTiO_3$ (JCPDS Card No. 22-153) is shown for comparison.

This indicates the starting of crystal-lization of the fiberlike sample at this heating temperature. With the increase of annealing temperature from 700 to 1000°C, the diffraction peaks become sharper and stronger due to the increase of the crystallinity and the growth of the crystallize size. For the sample annealed at 900 °C (Figure 1), well defined diffraction peaks can be indexed to the orthogonal phase of $CaTiO_3$ according to the JCPDS card (No. 22-153). No additional peaks for other phases were detected, indicating that Eu^{3+} ion have been effectively built into the $CaTiO_3$ host lattice without inducing significant changes of the crystal structure.

Fig. 2 shows the representative XRD patterns of $CaTiO_3$:xEu^{3+} (x = 4 mol %, 7 mol %, 10 mol %, 14 mol %, 18 mol %, 22 mol %, 26 mol %). It can be seen that it is well crystallized, and when the amount of Eu^{3+} is below 14mol%, it is in good agreement with JCPDS Card NO. 22-153. However, when the Eu^{3+} concentration reached 14mol%, Eu_2O_3 impurity phases can be found.
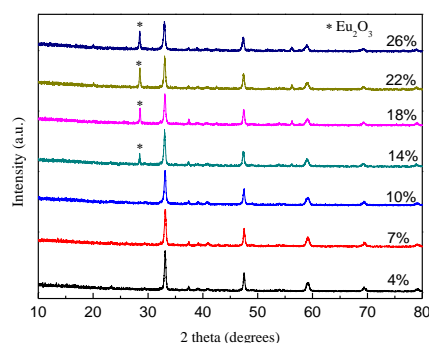
Fig. 2: Representative XRD patterns of $CaTiO_3$:xEu^{3+} (x = 4 mol %, 7 mol %, 10 mol %, 14 mol %, 18 mol %, 22 mol %, 26 mol %) nanofibers

3.2 Thermal Analysis

The precursor obtained by electrospinning was analyzed by TG-DTG. Figure 3 illustrates TG/DTG of PVP-Precursor in air atmosphere. The TG curve showed three steps in this

measurement and weight loss finished around 600℃。The sharp peaks appeared at 349, and 454 ^{o}C, corresponding to the decomposition of nitrates and the degradation of PVP, which has two degradation mechanisms involving both intra- and inter-molecular transfer reactions [14]**.** On the basis of the result from the TG-DTG analysis, the precursor was calcined from 600- 1000 ^{o}C.
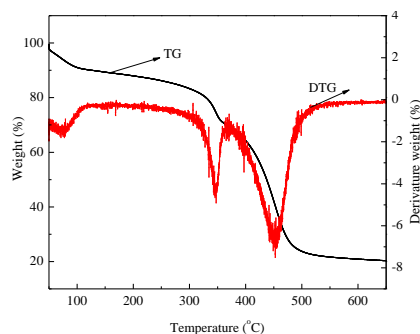
Fig. 3: TG-DTG curves of CaTiO$_3$: Eu^{3+} precursor.

3.3 SEM Images.

The morphologies of the final samples were investigated by SEM. Figure 4 presents the SEM images of CaTiO$_3$: Eu^{3+} nanofibers calcined at different temperatures. From Figure 3, we can see that after calcinations at high temperature, a well-defined fiber texture is maintained.
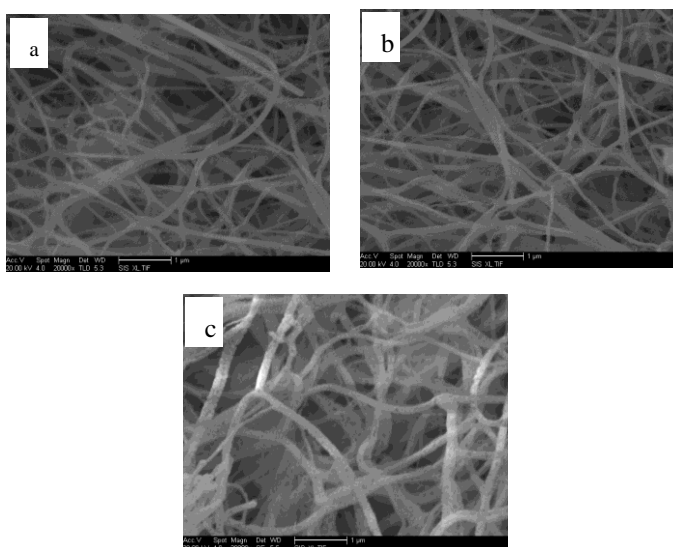
Fig. 4: SEM images of CaTiO$_3$: Eu^{3+} nanofibers calcined at (a) 700°C, (b) 800°C and (c) 900°C.

This indicates that the PVP backbone is introduced to encapsulate ceramic precursors in the dried green fiber. PVP is also introduced to achieve the required viscosity and mechanical properties in the green state. The calcined fibers are randomly distributed. The calcination makes the surface of fibers coarsen due to the removal of PVP and crystallization. The sintering temperature has an influence on both the crystalline phase and the surface morphology of the ceramic fibers. With the increase of the sintering temperature, the fibers turns coarsen and the grain size increases.

3.4. Luminescence properties

Fig. 5 depicts the photoluminescence excitation (PLE) spectra of the as-prepared $CaTiO_3$: $0.1Eu^{3+}$ phosphor. In the excitation spectrum monitored at 615 nm, the sample shows the excitation band from 370 to 420 nm with a maxium at 398 nm due to the $^7F_0 \rightarrow ^5L_6$ transition of the Eu^{3+} ions. The peaks at 365nm, 385nm and 420nm correspond to the $^7F_0 \rightarrow ^5D_4$, $^7F_0 \rightarrow ^5L_7$ and $^7F_0 \rightarrow ^5D_3$ transition of the Eu^{3+} ions.
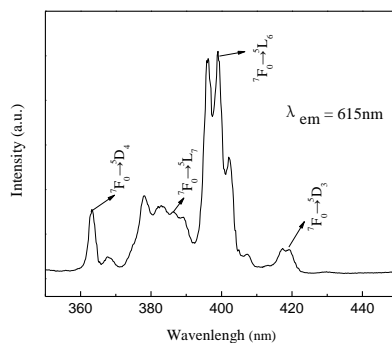
Fig. 5: PL spectra of $CaTiO_3$: $0.1Eu^{3+}$ phosphor

Upon excitation at 398 nm, the emission spectrum of $CaTiO_3$:Eu^{3+} sample are shown in Figure 6. It can be seen that the spectrum consists of the characteristic transition lines between Eu^{3+} levels. The emission spectrum exhibits three groups of emission lines at 589, 617nm, and 652nm which are assigned to the $^5D_0$-$^7F_1$, $^5D_0$-$^7F_2$ and $^5D_0$-$^7F_3$ transitions of Eu^{3+}, respectively. Obviously, the emission spectrum is dominated by the red $^5D_0$-$^7F_2$ (617 nm) transition of the Eu^{3+}, which is an electric-dipole-allowed transition and hypersensitive to the environment.

A series of phosphors with fixed Eu^{3+} molar content were prepared to study the effect of doping concentration on the luminescence properties of phosphors. Figure 6 shows the emission spectra of $CaTiO_3$:xEu^{3+} with different doping contents. The red emission of the Eu^{3+} increases gradually with the increase of Eu^{3+} concentration. Concentration quenching phenomenon was not observed in the solid solution range. According to the Dexter's energy transfer theory [14], concentration quenching is mainly caused by the nonradiative energy migration among the Eu^{3+} ions at the high concentration.
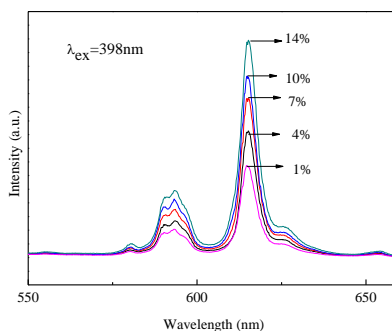
Fig. 6：   The emission spectra for $CaTiO_3$: xEu^{3+} (x = 1mol%, 4 mol%, 7 mol%, 10mol%, (e) 14 mol%) with various doped Eu^{3+} molar concentration

In order to investigate the effect of sintering temperature on luminescence properties, a series of CaTiO$_3$: Eu^{3+} naonfibers with different temperatures (600-1000°C) were synthesized. Figure 7 shows the emission spectra of CaTiO$_3$: Eu^{3+} nanofibers obtained at different temperatures. It can be seen that with the increase of the temperature, the emission intensity increases. At lower temperature, the pure CaTiO$_3$: Eu^{3+} can not be obtained, which resulted in the low the emission intensity. And it is consistent with the XRD results. The increase of temperature attribute to the increase of the emission intensity.
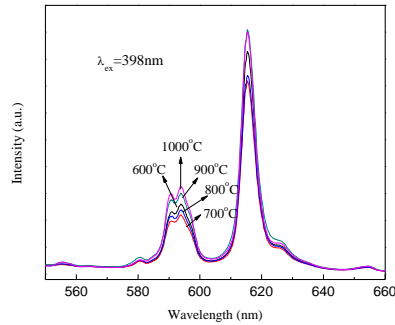
Fig. 7: PL spectra of CaTiO$_3$: Eu^{3+} nanofibers calcined at different temperatures

Fig. 8 shows the emission spectra of the as-prepared CaTiO$_3$: 0.07Eu^{3+} xGd^{3+} (x = 1 mol%, 2 mol%, 3 mol%, 4 mol%, 5 mol%) phosphor. It can be seen that under being excited at 398 nm, all characteristic peaks in emission spectra are attributed to Eu^{3+}, and the strongest peak locates at 615 nm. With the increase of Gd^{3+} concentration, the luminous intensity increased. However, when the concentration is above 4 mol%, the intensity then decreases. It indicates that the quenching concentration is 4 mol%. This is mainly due to the interaction between the dopant ions within the host lattice. The energy released in the form of heat, or the energy passed to the luminous center of Eu^{3+} reduction, which results in non-radiative transitions greater than radiative transitions, so the emission intensity of the samples decreased.
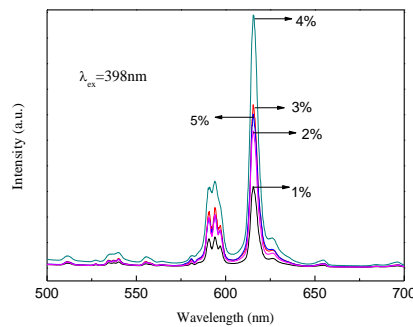
Fig. 8. PL spectra of spectra of CaTiO$_3$:0.07Eu^{3+}, xGd^{3+} (x = 1, 2, 3, 4, 5 mol%) nanofibers calcined at different temperatures

4. Conclusions

A series of $CaTiO_3$: Eu^{3+} nanofibers were synthesized by the electrospinning method, and the as-formed fibers are rough, and consist of nanoparticles. The increase of temperature attribute to the increase of the emission intensity. The obtained phosphors can be efficiently excited in the range from 370 to 420 nm. Under 398nm excitation, the phosphors show the characteristic emission of Eu^{3+}, i.e. ^5D_o-$^7F_1$、^5D_o-$^7F_2$、^5D_o-$^7F_3$ transitions, and the red emission intensity increases gradually with the increase of Eu^{3+} concentration. The further doping in $CaTiO_3$: Eu^{3+} nanofibers increases the emission intensity, and the optimum doping concentration is 4 mol%.

Acknowledgment

References

[1] Y. Jia, Y. Huang, Y. Zheng, N. Guo, H. Qiao, Q. Zhao, W. Lv, H.P. You, J. Mater. Chem. **22**, 15146 (2012).

[2] J. K. Li, J. G. Li, S. H. Liu, X. D. Li, X. D. Sun, Y. Sakka, J. Mater. Chem. C, **1**, 7614 (2013).

[3] C. H. Huang, T. M. Chen, Inorg. Chem., **50**, 5725 (2011).

[4] C. K. Chang, T. M. Chen, Appl. Phys. Lett. **90**, 161901 (2007).

[5] W. Lu, N. Guo, Y. C. Jia, Q. Zhao, W. Z. Lv, M. M. Jiao, B. Q. Shao, H. P. You, Inorg. Chem., **52**, 3007 (2013).

[6] H.S. Kim, K. Machida, T. Horikawa, H. Hanzawa, J. Alloys Compd. **633**, 97e103 (2015).

[7] Q.F. Wang, Y. Liu, Y. Wang, W.X. Wang, Y. Wan, G.G. Wang, Z.G. Lu, J. Alloys Compd. **625,** 355e361 (2015).

[8] B. Wang, H. Lin, J. Xu, H. Chen, Z. Lin, F. Huang, and Y.S. Wang，Inorg. Chem. **54**, 11299 (2015).

[9] B. Lokesh, N. M. Rao, J Mater Sci: Mater Electron, DOI 10.1007/s10854-016-4290-2.

[10] M. K. Mahata, K. Kumar, V. K. Rai, Spectrochimica Acta Part A: Molecular and Biomolecular Spectroscopy **124**, 285 (2014).

[11] M.Saif, M.Shebl, A.Mbarek, Al Nabeel, R. Maalej, R. Shokry, Journal of Photochemistry and Photobiology A: Chemistry **301**, 1 (2015)

[12] L. Pieterson, S. Soverna, A. Meijerink, J Electrochem Soc., **147**, 4688 (2000).

[13] S.J. Azhari, M.A. Diab, Polym. Degrad. Stab. **60**, 253 (1998).

[14] Y. E. Lee, D. P. Norton, J. D. Budai, Appl Phys Lett **77**, 678 (2000).